*Semiconductor Physics, Quantum Electronics & Optoelectronics, 2025. V. 28, No 2. P. 221-231.*

*Optoelectronics and optoelectronic devices*

# Calculation of atomic structure of neutral vanadium

**S.V. Gedeon*, V.Yu. Lazur, A.A. Kochemba**

*Uzhhorod National University, Department of Theoretical Physics*
*53 Voloshina Street, 88000 Uzhhorod, Ukraine*
**Corresponding author e-mail: sergej.gedeon@uzhnu.edu.ua*

**Abstract.** Multi-configuration Hartree–Fock method combined with configuration interaction approach with non-orthogonal orbitals and *B*-splines as basis functions are employed to study the atomic structure of neutral vanadium. The energy levels of the ground and 44 lower excited states are calculated both within the non-relativistic *LS* approximation and with relativistic corrections within the Breit–Pauli approach. The calculation results have a satisfactory agreement with the available experimental data. The obtained sets of wave functions can be used in the subsequent study of photoionization and electron scattering on vanadium atoms.

**Keywords:** vanadium atom, atomic structure, electronic correlation, configuration interaction, non-orthogonal orbitals.

https://doi.org/10.15407/spqeo28.02.221
PACS 31.15.v–

Manuscript received 22.11.24; revised version received 15.02.25; accepted for publication 11.06.25; published online 26.06.25.

## 1. Introduction

The study of spectroscopic properties and structure of vanadium atomic systems is of great interest to many branches of applied and fundamental science.

The study of transition metals, including vanadium, has long been an important problem of astrophysics. Due to the large binding energy per nucleon and the peculiarities of nucleosynthesis processes in supernovae, transition elements are more abundant in space than would be expected according to general trends. In particular, the cosmic abundance of elements from Sc to Ni ($21 \leq Z \leq 28$) forms a peculiar peak around iron. Moreover, partially filled 3*d*-shells in the atomic structure of such elements lead to spectra with a large number of lines, making transition elements particularly interesting for astrophysics. On the other hand, due to the specific structure of the nuclei, elements with even atomic numbers are much more abundant than elements with odd ones (the so-called Oddo–Harkins rule). Therefore, it is no wonder that the spectra of such elements as Ti, Cr, Fe, Ni ($Z$ = 22, 24, 26 and 28, respectively) have been studied much more than the spectra of adjacent Sc, V, Mn and Co ($Z$ = 21, 23, 25, 27). This is indirectly evidenced by the complete absence of data on vanadium in one of the widely used atomic databases for spectroscopic diagnostics of astrophysical plasma CHIANTI [1].

Accurate values of the element abundance are the key components needed to understand the chemical evolution of stars and galaxies [2–4]. Obtaining reliable abundance values requires accurate atomic data, including ionization cross sections, oscillator strengths, and transition probabilities [5, 6].

The transition probabilities and other characteristics are usually better investigated for resonance lines and stronger transitions. On the other hand, there are also a large number of weak lines in the spectra of 3*d*-elements. There are often too few measurements for such lines to compare with the data from other independent experiments, and sometimes the results of such measurements are absent at all. For example, in the experimental work [7], hyperfine structure of weak lines in the spectrum of neutral vanadium was studied. In this study, the values of the magnetic dipole hyperfine structure constant $A$ were measured for 36 levels of the vanadium atom, and 29 of these values were obtained for the first time.

For modelling stellar atmospheres in non-local thermodynamic equilibrium, it is important to take into account all important inelastic processes occurring with the atom or ion of interest. This requires quantifying the efficiency of a large number of such processes to determine whether they are important or not. At the same time, a significant part of the weak lines of the solar spectrum requires further study, and even the simplest estimates for forbidden transitions require knowledge of wave functions [8].

Therefore, the results of theoretical calculations (especially for weak lines) can be used for both validation of existing experimental values and as an important complement for transitions not yet measured in the laboratory.

In addition to the interest in vanadium by astrophysics, its alloys are widely used as heat-resistant and anti-corrosion materials for industrial devices. Spectral lines of neutral and ionized vanadium are observed in the plasma formed during laser treatment of surfaces coated with such alloys (see *e.g.* references in the review [9]). Therefore, determination of the spectroscopic properties of vanadium atom is relevant not only for the diagnostics of plasma in stellar atmospheres, but also for the analysis of plasma in industrial processes. Moreover, not only resonant but also weak forbidden M1 transitions are of interest [10].

Optical emission spectroscopy studies of vanadium plasma in a cathodic-arc discharge in a nitrogen atmosphere have been carried out in the recent work [11]. In scope of that research, the spectral lines of neutral atoms and ions of the cathode material V I, V II, and V III were observed in the discharge plasma.

Vanadium alloys are also promising as blanket structural materials for fusion power systems. They have low induced activation characteristics, high temperature strength and high thermal stress factors. Recent research has successfully solved many critical problems and increased the possibility of using vanadium alloys as structural materials for fusion reactors [12]. Modern studies also confirm the persistent interest in such alloys [13, 14].

In addition to the wide use of vanadium in construction of high-temperature devices, this material is also used as an active medium of gas lasers. The first observations of laser generation at the transitions of vanadium atoms are described in [15, 16]. It was reported there that lasers with the wavelengths of 409.5, 560.4, 575.3, 581.7, and 637.9 nm were obtained by optical pumping of vanadium vapors. A more detailed study of the processes occurring in such lasers is carried out in [17]. Also, the work [18] provides a thorough review of experiments on generation of higher harmonics using vanadium as a nonlinear medium.

Existence of a wide range of astrophysical and laboratory observations requires complex theoretical models to interpret the measurement results and a large amount of input data for these models. As mentioned above, such atomic data include, in particular, excitation rates, photoionization cross sections, oscillator strengths, transition probabilities, energy levels and line wavelengths. Although some of these data can be obtained experimentally, they are usually not accurate enough or limited to a small number of transitions.

Atomic structures that have open shells with several equivalent *d*-electrons are of particular interest for theoretical study, since the systems of this type demonstrate characteristics intermediate in complexity between the well-studied *s*- and *p*-elements and very complex rare-earth elements, whose structures are dominated by the *f*-electronic configurations. The vanadium atom, which has an open *d*-shell, also belongs to such transitional elements. The study of transition elements requires development of new and improvement of existing methods of calculating the atomic structure and elementary processes of electron and photon scattering on atoms.

One of the effective methods for systematic calculations of electron and photon scattering processes by complex atoms is the *B*-spline *R*-matrix method (BSR) [19]. The main advantages, features and examples of the application of the BSR method to the study of specific atomic systems and processes are given, in particular, in our recent works [20–22]. Also, with a change in the boundary conditions, the BSR method can be used to calculate the wave functions of bound states of multi-electron atomic systems. The examples of successful use of the BSR method for this type of problems can be found e.g. in [23–26]. In general, application of the BSR method allows obtaining extensive data sets for various characteristics of elastic and inelastic scattering processes, which are necessary for modeling astrophysical and laboratory plasmas.

An important component of the application of this method is availability of reliable wave functions for accurate description of an atomic target. Multi-configuration Hartree–Fock (MCHF) method combined with configuration interaction (CI) methods are a method of choice for complex atoms where atomic state functions are expanded in a basis of configuration state functions [27]. At the same time, existing theoretical studies of the atomic structure of vanadium either describe too complex calculations, which are necessary to determine more sensitive atomic characteristics, or use simplified models that are sufficient only to describe specific processes.

Thus, in [28], a non-relativistic MCHF approximation was used to calculate the hyperfine structure of the ground state of a neutral vanadium atom. The influence of all types of correlation effects on the magnetic dipole hyperfine factor $A$ and the electric quadrupole factor $B$ has been investigated in detail. The number of configurations in multi-configuration expansions with different sets of correlation orbitals ranged from several hundreds to tens of thousands. Obviously, use of such wave functions to describe the target states in scattering calculations is currently not possible due to existing computational limitations. In [29], within the framework of the configuration interaction method, the impact of correlation effects on the excitation energy of the lower excited state of neutral vanadium was investigated. Accordingly, only the calculations of the wave functions of the two lowest states of neutral vanadium, namely the ground $3d^3 4s^2\ ^4F$ and the excited $3d^4 4s\ ^6D$ state, were considered in detail.

A large number of calculations for interpretation of spectroscopic data for neutral vanadium have been performed using the Hartree–Fock method with relativistic corrections (HFR) [30] and semi-empirical fitting. In particular, the work [31] presented and classified the energy levels of neutral vanadium, which correspond to 198 even and 346 odd terms. In [9], the parameters of 35 spectral lines from the ultraviolet and blue part of the spectrum were calculated. A detailed review of the most relevant experimental and theoretical studies on energy levels, spectral lines and transition probabilities for neutral vanadium is also given in [32].

At the same time, there is a limited number of studies of electron scattering processes on vanadium atom. For example, experimental cross-sections of excitation of several levels of neutral vanadium are given in [33, 34] and earlier works [35, 36]. Theoretical calculations of scattering cross sections are presented in [37].

The purpose of the present work is to obtain the wave functions of the ground and lower excited states of a neutral vanadium atom for their further use in systematic scattering calculations using modern computational approaches such as the *B*-spline *R*-matrix method.

## 2. Computational methods

A neutral vanadium atom with nuclear charge $Z = 23$ has electronic configuration of the ground state $[\mathrm{Ar}]3d^3 4s^2\ {}^4F$, *i.e.* five electrons over argon-like core and an open *d*-shell. The observed energy levels of the exited states of neutral vanadium atom V I belong to two configuration systems in scope of the *LS*-coupling scheme. The "normal" or "singly excited" system consists of $3d^4({}^M L)nl$ subconfigurations, which are built on the parent terms $({}^M L)$ in V II. The subconfigurations $3d^3({}^M L)4snl$ in the "doubly excited" system are built on the $({}^M L)$ grandparent terms in V III [31]. Such complex electronic structure of the vanadium atomic system leads to high number of the *LS* terms.

In particular, according to the NIST data [38], many doublet, quartet and sextet levels were identified in the energy spectrum of neutral vanadium. In the *LS* coupling scheme those levels have electronic configurations $3d^3 4snl$ ($n = 4, 5$, $l = 0$–2), $3d^4 nl$ ($n = 4, 5$, $l = 0 - 2$), $3d^5$, $3d^2 4s^2 4p$ and $3d^4 6s$ with different even $({}^6S^{2,4,6}PDFGH^2I)$ and odd $({}^{2,4,6}SPDFG^{2,4}HI^{\circ})$ terms.

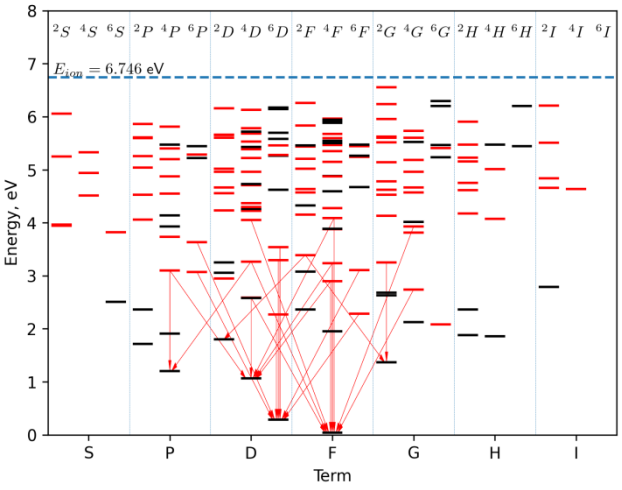


**Fig. 1.** Energy levels diagram of vanadium atom according to the NIST data [38]. The energies for multiplets are averaged over the fine structure levels. Black dashes correspond to even terms, red dashes – odd terms. Arrows indicate the main allowed transitions between the levels. The levels are grouped according to the total orbital angular momentum *L* and the multiplicity $2S+1$ of the terms in the *LS* coupling approximation.

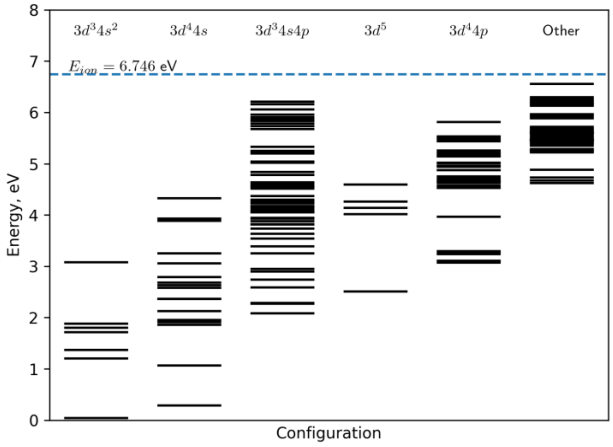


**Fig. 2.** Energy levels diagram of vanadium atom according to the NIST data [38]. The energies for multiplets are averaged over the fine structure levels. The levels are grouped according to the electronic configuration of the atomic states in the *LS* coupling approximation.

A schematic diagram of the energy levels of neutral vanadium (weighted average for multiplets) is shown in Fig. 1. The figure also shows the main allowed transitions between the levels in the lower part of the energy spectrum.

Fig. 2 shows the main electronic configurations that correspond to different terms in the *LS* coupling scheme. The lowest levels with configurations $3d^3 4s^2$, $3d^4 4s$, $3d^5$ and $3d^4 4p$ often overlap with each other and thus may have strong configuration interaction. The effects of electron correlation between valence 3*d*, 4*s* and 4*p* electrons can also be significant.

Accurate representation of electron correlation effects in atomic systems with open 3*d*-shell requires inclusion of one- and two-electron excitations from the valence to the excited orbitals in the CI-expansions. This leads to the large multi-configuration expansions, the convergence of which becomes slower because of term-dependence of the valence orbitals. One of the possible approaches to avoid this is to use non-orthogonal orbitals. This allows one to decrease the size of the multi-configuration expansions and does not create any restrictions for further use of the obtained wave functions in scattering calculations using the *B*-spline *R*-matrix method.

To calculate the wave functions of the ground and excited states of vanadium atom, we employed a multi-configuration Hartree–Fock method [39] together with a CI approach with non-orthogonal orbitals and *B*-splines as basis functions [40, 41]. This approach makes it possible to flexibly and effectively take into account the term-dependence of the valence orbitals, and the correlation and relaxation effects. Such efficiency is also achieved through the correct selection of dominant configurations from hundreds or thousands of individual atomic configurations formed by all possible one- and two-electron excitations of valence 3*d*, 4*s* and 4*p* orbitals of the considered configuration. By analyzing the full configuration expansion for each considered term and selecting

only configurations with significant mixing coefficients, it is possible to obtain final multi-configuration expansions that include all important electronic correlations and at the same time have a controlled size, which is important for further scattering calculations.

First, we generated spectroscopic orbitals 1*s*, 2*s*, 2*p*, 3*s*, 3*p*, 3*d* and 4*s* for the ground state $3d^3 4s^2\,{}^4F$ of neutral vanadium using the Hartree–Fock method. Later, deep core orbitals 1*s*, 2*s*, and 2*p* were used for all other states. At the same time, sub-valence orbitals 3*s* and 3*p* together with valence 3*d*, 4*s* and 4*p* orbitals were calculated separately for different configurations. They were obtained from term-average Hartree–Fock-calculations for each of the principal electronic configurations. Such optimization has made it possible to take into account term-dependence of the valence 3*d*, 4*s* and 4*p* orbitals. For the wave functions calculated in our research, the average radius of the 3*d*-orbital was equal to 1.88, 1.56, 1.51, 1.35, and 1.34 a.u. for the $3d^5$, $3d^4 4s$, $3d^4 4p$, $3d^3 4s^2$, and $3d^3 4s 4p$ configurations, respectively. This fact clearly demonstrates the importance of the term-dependence of the valence orbitals.

The spectroscopic orbitals mentioned above were supplemented by sets of correlation orbitals 4*l* and 5*l* ($l$ = 0 – 4). The correlation orbitals were obtained in separate MCHF calculations for one of the terms for each of the selected configurations. Subsequently, the obtained sets of the correlation orbitals were used in the calculations of all other terms with the same configuration. In the calculations of each of the sets of correlation orbitals, one- and two-electron excitations from the outer shells were included in the multi-configuration expansions. As mentioned in [28], taking into account all the single and selected double substitutions allows one to describe successfully even the hyperfine structure splitting. Also in [42], it is indicated in research of chromium ion Cr II, which is isoelectronic to neutral vanadium, that inclusion of excitations from inner 3*s* and 3*p* shells should not affect the relative position of the levels, and we made the same assumption in our investigation.

The configurations with the mixing coefficients less than 0.001 were excluded from the final CI-expansions. Such a cut-off parameter allowed us to reduce the size of CI-expansions to ~30–650 configurations for all the atomic states under consideration in the *LS* approximation. This is considered sufficient to include main correlation effects with the relatively small number of configurations.

Finally, we obtained the *J*-dependent atomic states by diagonalizing the Breit–Pauli Hamiltonian on the basis of the multi-configuration *LS* wave functions described above, using the CI approach with non-orthogonal orbitals [40]. In the present calculations, we included all the one-body operators in the Breit–Pauli Hamiltonian, namely relativistic mass correction, one-body Darwin and spin-orbit operators.

The final multi-configuration expansions contain about 350 configurations on average. Therefore, they can be used in scattering calculations using the available computational resources.

## 3. Results and discussion

As a result of the calculations, we obtained the wave functions of the ground and 44 excited states of neutral vanadium atom, which have electronic configurations $3d^3 4s^2$, $3d^4 4s$, $3d^3 4s 4p$, $3d^5$ and $3d^4 4p$ and terms ${}^{2,4}PDFGH^2I^6SD$ and ${}^{2,6}S^{4,6}PDFG^o$.

In Table 1 and Fig. 3, we present comparison of the excitation energies, calculated by us in scope of the non-relativistic *LS* approximation with experimental energies, recommended by NIST [38] (weighted average for the fine structure levels). The overall agreement between the theoretical and experimental values is satisfactory with the median value of the energy difference equal to about ~0.5 eV. The last column of the table shows the number of configurations in the multi-configuration expansion for each state. The maximum number of possible configurations for a given term and with selected restrictions for one- and two-electron excitations from the valence shells is displayed in parentheses. Some particular states from the upper part of the energy spectrum were not included in the present research due to the computational procedure features of the chosen approach. For these terms, only the experimental excitation energies are shown in the table. The chart also shows that for the terms $b\,{}^4D$, $b\,{}^2G$ and ${}^4F$ of the $3d^4 4s$ configuration, the excitation energy is significantly increased after cutting off configurations with small coefficients in the multi-configuration expansion. It is certain that these terms require separate investigation and detailed analysis of possible ways to include term-dependency of valence orbitals, effects of correlation and relaxation.

To study convergence of the multi-configuration expansions, we performed additional calculations with a cut-off parameter for the expansion coefficients equal to 0.01. After that, the number of configurations in the expansions decreased to ~10…100, but the deviation of the excitation energies from the experimental values accordingly increased by ~0.1 eV on average, which

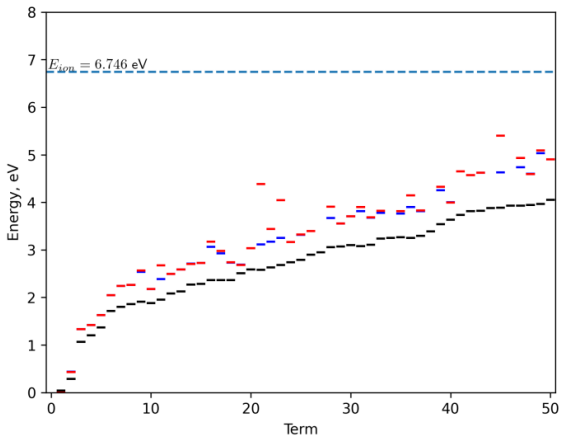


**Fig. 3.** Comparison of excitation energies. Black dashes – experimental energies, recommended by NIST [38]; blue dashes – present calculations, full CI-expansion; red dashes – present calculations, CI-expansion with the mixing coefficients > 0.001.

**Table 1.** Excitation energies of the lower states of vanadium atom.

| | Configuration | Term | $E_{exc}$ [38], eV | $E_{exc}$ MCHF, eV | $\Delta E_{exc}$, eV | $N_{conf}$ |
|---|---|---|---|---|---|---|
| 1 | $3d^3 4s^2$ | a $^4F$ | 0.040 | 0.000 | | 302 (934) |
| 2 | $3d^4[^5D]4s$ | a $^6D$ | 0.285 | 0.433 | 0.148 | 116 (176) |
| 3 | $3d^4[^5D]4s$ | a $^4D$ | 1.066 | 1.332 | 0.267 | 274 (803) |
| 4 | $3d^3 4s^2$ | a $^4P$ | 1.205 | 1.418 | 0.213 | 328 (610) |
| 5 | $3d^3 4s^2$ | a $^2G$ | 1.365 | 1.629 | 0.264 | 388 (1206) |
| 6 | $3d^3 4s^2$ | a $^2P$ | 1.712 | 2.044 | 0.332 | 381 (789) |
| 7 | $3d^3 4s^2$ | $^2D2$ | 1.802 | 2.243 | 0.441 | 512 (1156) |
| 8 | $3d^4[^3H]4s$ | a $^4H$ | 1.859 | 2.265 | 0.406 | 274 (685) |
| 9 | $3d^4[^3P2]4s$ | b $^4P$ | 1.908 | 2.567 | 0.659 | 337 (610) |
| 10 | $3d^3 4s^2$ | a $^2H$ | 1.884 | 2.175 | 0.291 | 322 (976) |
| 11 | $3d^4[^3F2]4s$ | b $^4F$ | 1.950 | 2.676 | 0.726 | 313 (934) |
| 12 | $3d3[^4F]4s4p[^3P^o]$ | z $^6G^o$ | 2.082 | 2.493 | 0.411 | 169 (381) |
| 13 | $3d^4[^3G]4s$ | a $^4G$ | 2.128 | 2.591 | 0.463 | 351 (823) |
| 14 | $3d^3[^4F]4s4p[^3P^o]$ | z $^6D^o$ | 2.268 | 2.704 | 0.437 | 231 (384) |
| 15 | $3d^3[^4F]4s4p[^3P^o]$ | z $^6F^o$ | 2.287 | 2.722 | 0.434 | 223 (403) |
| 16 | $3d^4[^3P2]4s$ | b $^2P$ | 2.363 | 3.175 | 0.812 | 378 (789) |
| 17 | $3d^4[^3H]4s$ | b $^2H$ | 2.367 | 2.980 | 0.613 | 346 (976) |
| 18 | $3d^4[^3F2]4s$ | a $^2F$ | 2.363 | 2.741 | 0.378 | 586 (1267) |
| 19 | $3d^5$ | a $^6S$ | 2.505 | 2.679 | 0.174 | 27 (49) |
| 20 | $3d^3[^4F]4s4p[^3P^o]$ | z $^4D^o$ | 2.586 | 3.033 | 0.447 | 606 (1731) |
| 21 | $3d^4[^3D]4s$ | b $^4D$ | 2.578 | 4.387 | 1.809 | 274 (803) |
| 22 | $3d^4[^3G]4s$ | $^2G$ | 2.628 | 3.437 | 0.809 | 416 (1206) |
| 23 | $3d^4[^1G2]4s$ | b $^2G$ | 2.681 | 4.044 | 1.363 | 416 (1206) |
| 24 | $3d3[^4F]4s4p[^3P^o]$ | z $^4G^o$ | 2.741 | 3.166 | 0.426 | 561 (1790) |
| 25 | $3d^4[^1I]4s$ | $^2I$ | 2.788 | 3.320 | 0.532 | 264 (706) |
| 26 | $3d^3[^4F]4s4p[^3P^o]$ | z $^4F^o$ | 2.894 | 3.397 | 0.502 | 621 (1859) |
| 27 | $3d^3[^4F]4s4p[^3P^o]$ | z $^2D^o$ | 2.951 | | | – (2279) |
| 28 | $3d^4[^3D]4s$ | $^2D$ | 3.054 | 3.906 | 0.851 | 517 (1156) |
| 29 | $3d^4[^5D]4p$ | z $^6P^o$ | 3.070 | 3.551 | 0.481 | 88 (116) |
| 30 | $3d^4[^5D]4p$ | z $^4P^o$ | 3.099 | 3.702 | 0.603 | 222 (566) |
| 31 | $3d^3 4s^2$ | $^2F$ | 3.076 | 3.900 | 0.824 | 644 (1267) |
| 32 | $3d^4[^5D]4p$ | y $^6F^o$ | 3.107 | 3.683 | 0.576 | 112 (182) |
| 33 | $3d^4[^5D]4p$ | y $^4F^o$ | 3.234 | 3.822 | 0.587 | 352 (906) |
| 34 | $3d^3[^4F]4s4p[^3P^o]$ | z $^2G^o$ | 3.249 | | | – (2420) |
| 35 | $3d^4[^5D]4p$ | y $^4D^o$ | 3.269 | 3.813 | 0.544 | 365 (860) |
| 36 | $3d^4[^1D2]4s$ | $^2D$ | 3.248 | 4.147 | 0.899 | 517 (1156) |
| 37 | $3d^4[^5D]4p$ | y $^6D^o$ | 3.297 | 3.829 | 0.532 | 122 (188) |
| 38 | $3d^3[^4F]4s4p[^3P^o]$ | z $^2F^o$ | 3.391 | | | – (2557) |
| 39 | $3d^3[^4P]4s4p[^3P^o]$ | x $^6D^o$ | 3.543 | 4.328 | 0.784 | 231 (384) |
| 40 | $3d^3[^4P]4s4p[^3P^o]$ | y $^6P^o$ | 3.636 | 3.997 | 0.361 | 211 (258) |
| 41 | $3d^3[^4P]4s4p[^3P^o]$ | y $^4P^o$ | 3.731 | 4.651 | 0.920 | 581 (1157) |
| 42 | $3d^3[^2G]4s4p[^3P^o]$ | y $^4G^o$ | 3.814 | 4.574 | 0.760 | 561 (1790) |
| 43 | $3d^3[^4P]4s4p[^3P^o]$ | z $^6S^o$ | 3.823 | 4.619 | 0.796 | 70 (103) |
| 44 | $3d^3[^2G]4s4p[^3P^o]$ | x $^4F^o$ | 3.877 | | | – (1859) |
| 45 | $3d^4[^3F1]4s$ | $^4F$ | 3.888 | 5.402 | 1.514 | 313 (934) |
| 46 | $3d^3[^4F]4s4p[^3P^o]$ | x $^4G^o$ | 3.930 | | | – (1790) |
| 47 | $3d^4[^3P1]4s$ | $^4P$ | 3.928 | 4.936 | 1.008 | 337 (610) |
| 48 | $3d^3[^2P]4s4p[^3P^o]$ | $^2S^o$ | 3.941 | 4.596 | 0.655 | 346 (565) |
| 49 | $3d^4[^3P2]4p$ | y $^2S^o$ | 3.963 | 5.088 | 1.125 | 162 (290) |
| 50 | $3d^3[^2P]4s4p[^3P^o]$ | x $^4D^o$ | 4.052 | 4.902 | 0.850 | 606 (1731) |

**Table 2.** Dependence of the deviation of the excitation energies on the number of configurations included in the CI-expansion.

| Configuration | | MCHF | | | MCHF 0.001 | | | MCHF 0.01 | | |
|---|---|---|---|---|---|---|---|---|---|---|
| | | $\Delta E_{exc}$, eV | $\Delta E_{exc}/E_{NIST}$, % | $N_{conf}$ | $\Delta E_{exc}$, eV | $\Delta E_{exc}/E_{NIST}$, % | $N_{conf}$ | $\Delta E_{exc}$, eV | $\Delta E_{exc}/E_{NIST}$, % | $N_{conf}$ |
| $3d^34s^2$ | min | 0.215 | 15.411 | 610 | 0.213 | 15.471 | 302 | 0.274 | 16.159 | 41 |
| | max | 0.735 | 24.256 | 1267 | 0.824 | 26.782 | 644 | 1.208 | 39.250 | 93 |
| | median | 0.312 | 19.314 | 976 | 0.312 | 19.388 | 381 | 0.356 | 23.230 | 58 |
| $3d^44s$ | min | 0.153 | 15.475 | 176 | 0.148 | 15.995 | 116 | 0.170 | 22.010 | 33 |
| | max | 0.809 | 53.719 | 1267 | 1.809 | 70.189 | 586 | 3.568 | 133.095 | 96 |
| | median | 0.542 | 21.383 | 823 | 0.726 | 27.873 | 337 | 1.344 | 59.379 | 65.5 |
| $3d^34s4p$ | min | 0.366 | 10.057 | 103 | 0.361 | 9.918 | 70 | 0.361 | 11.499 | 29 |
| | max | 0.801 | 20.958 | 2557 | 0.920 | 24.653 | 621 | 1.287 | 34.486 | 99 |
| | median | 0.437 | 19.379 | 1731 | 0.436 | 18.179 | 346 | 0.455 | 18.236 | 64.5 |
| $3d^5$ | min | 0.180 | 7.196 | 49 | 0.174 | 6.958 | 27 | 0.063 | 2.533 | 12 |
| | max | –//– | –//– | –//– | –//– | –//– | –//– | –//– | –//– | –//– |
| | median | –//– | –//– | –//– | –//– | –//– | –//– | –//– | –//– | –//– |
| $3d^44p$ | min | 0.486 | 15.155 | 116 | 0.481 | 15.677 | 88 | 0.387 | 12.612 | 29 |
| | max | 1.071 | 27.036 | 906 | 1.125 | 28.393 | 365 | 1.156 | 29.169 | 78 |
| | median | 0.547 | 16.904 | 290 | 0.576 | 18.158 | 162 | 0.587 | 17.954 | 44 |
| Total | min | 0.153 | 7.196 | 49 | 0.148 | 6.958 | 27 | 0.063 | 2.533 | 12 |
| | max | 1.071 | 53.719 | 2557 | 1.809 | 70.189 | 644 | 3.568 | 133.095 | 99 |
| | median | 0.524 | 19.932 | 883 | 0.560 | 20.368 | 337 | 0.651 | 26.232 | 59 |

corresponds to ~5 percentage points when comparing to the relative values. A comparison of the deviations of the excitation energies from the experimental values depending on the number of configurations in the expansion is presented in Table 2. Note, that the results in the table illustrate only a general tendency of convergence for each set of configurations, *i.e.*, the minimum and maximum values for different approximations do not necessarily correspond to the same terms within the specified set. The obtained data indicate both the similarity of convergence patterns of multi-configuration expansions for each type of configurations under consideration as well as certain differences for specific terms that require further investigation.

In particular, for the states with configuration $3d^34s^2$, the minimum and median values of the deviation are ~0.2 and ~0.3 eV, respectively, for the states $3d^34s4p$ – 0.36 and 0.44 eV, while for the states $3d^44s$– 0.15 and 0.7 eV. We noticed during the calculation process that the $3d^44s$ states demonstrated both high sensitivity to the one-electron orbitals selection and slow convergence of the multi-configuration expansion.

A normal practice for more accurate account of correlation effect for the terms with different convergence patterns is to use different cut-off parameters for the coefficients of the multi-configuration expansions (see *e.g.* [42]). Usually, this procedure allows one to improve the difference between the calculated levels of excitation energies, which is important for further scattering calculations. Such fitting procedure was not performed in scope of the present research.

Table 3 shows the main configurations with the most important correlation configurations and their mixing coefficients in the final CI-expansions for selected terms. The correlation orbitals have average radii close to the outer 3*d*, 4*s* and 4*p* valence orbitals of the corresponding configurations. Obviously, the correlation patterns are different for different types of configurations. But the common trend is $3d^2$–$4d^2$ and $3d^2$–$5d^2$ substitutions along with the other two-electron excitations from the 3*d* shell: $3d^2$–$4p^2$ and $3d^2$–$4f^2$. These two-electron excitations exhibit the 3*d* inner-shell correlation and are expected to be different for the considered $3d^34s^2$, $3d^44l$ and $3d^5$ configurations because of the different numbers of 3*d* electrons. For the $3d^44s$ configurations, it is important to include the correlation configurations $3d^24s5d^2$ and $3d^24s4d5d$. The states $3d^34s^2$ are strongly mixed with the $3d^34p^2$ and $3d^44s$ configurations.

**Table 3.** Correlation configurations and their mixing coefficients for the primary configurations of vanadium atom.

| Primary configuration | Correlation configuration | Coefficient | Primary configuration | Correlation configuration | Coefficient |
|---|---|---|---|---|---|
| $3d^34s^2$ | $3d^34p^2$ | 0.197 | $3d^34s4p$ | $3d^34s5p$ | 0.143 |
| | $3d^44s$ | 0.101 | | $3d^34p4d$ | 0.053 |
| | $3d^24s4p^2$ | 0.066 | | $3d^34p4d$ | 0.043 |
| | $3d^34s5s$ | 0.045 | | $3d^34p4d$ | 0.043 |
| | $3d^24s4p4f$ | 0.037 | | $3d^24s4d5p$ | 0.038 |
| | $3d^24s4p^2$ | 0.034 | | $3d^24p^24f$ | 0.032 |
| | $3d^5$ | 0.034 | | $3d^34d5p$ | 0.030 |
| | $3d^24s4d5s$ | 0.031 | | $3d^24p4d5s$ | 0.027 |
| | $3d^24s4p4f$ | 0.031 | | $3d^34p5s$ | 0.024 |
| | $3d^34s4d$ | 0.031 | | $3d^24s4p4d$ | 0.023 |
| | $3d^44d$ | 0.028 | | $3d^24s4d4f$ | 0.023 |
| | $3d^24s4d5s$ | 0.026 | | $3d^24s4d5p$ | 0.023 |
| | $3d^24s4p4f$ | 0.026 | | $3d^24s4d5p$ | 0.020 |
| | $3d^34d^2$ | 0.025 | | | |
| | $3d^44s$ | 0.025 | $3d^5$ | $3d^34d^2$ | 0.140 |
| | $3d^35s^2$ | 0.024 | | $3d^34d^2$ | 0.129 |
| | $3d^24s^24d$ | 0.024 | | $3d^34p^2$ | 0.076 |
| | $3d^34s4d$ | 0.024 | | $3d^35d^2$ | 0.020 |
| | | | | | |
| $3d^44s$ | $3d^24s5d^2$ | 0.070 | $3d^44p$ | $3d^34s4p$ | 0.604 |
| | $3d^45s$ | 0.059 | | $3d^34s5p$ | 0.274 |
| | $3d^24s5d^2$ | 0.049 | | $3d^24s4p4d$ | 0.091 |
| | $3d^24s5d^2$ | 0.048 | | $3d^45p$ | 0.091 |
| | $3d^34p4f$ | 0.045 | | $3d^34p5s$ | 0.083 |
| | $3d^24s4d5d$ | 0.043 | | $3d^24s4p4d$ | 0.065 |
| | $3d^35s5d$ | 0.040 | | $3d^24s4p4d$ | 0.055 |
| | $3d^24s4f^2$ | 0.034 | | $3d^34p4d$ | 0.045 |
| | $3d^24s5d^2$ | 0.033 | | $3d^24s4d5p$ | 0.041 |
| | $3d^24s4f^2$ | 0.031 | | $3d^34d5p$ | 0.040 |
| | $3d^34s5d$ | 0.030 | | $3d^24s4p4d$ | 0.036 |
| | $3d^24s4p^2$ | 0.030 | | $3d^34d5p$ | 0.033 |
| | $3d^24s4p^2$ | 0.030 | | $3d^34p4d$ | 0.029 |
| | $3d^24s4f^2$ | 0.029 | | $3d^34d5p$ | 0.029 |
| | $3d^34p4f$ | 0.026 | | $3d^24s4p5d$ | 0.027 |
| | $3d^24s4d5d$ | 0.024 | | $3d^34s4f$ | 0.025 |
| | $3d^24s4d^2$ | 0.024 | | $3d^34p4d$ | 0.024 |
| | $3d^34p4f$ | 0.022 | | $3d^34d5p$ | 0.020 |
| | $3d^35s5d$ | 0.022 | | | |
| | $3d^24s4d5d$ | 0.022 | | | |

**Note:** duplicated correlation configurations for the same set have different intermediate terms for the equivalent electrons.

As one can see from Table 3, the electronic correlation effects due to the 3*d*–4*f* excitation are also significant. The large correlation contributions of the correlated 4*f* orbitals are caused by the proximity of radii of the correlated 4*f* and valence 3*d* orbitals. It is important to notice that the small radius of the correlated *f*-orbitals combined with the large number of configurations that include these orbitals can lead to non-physical effects while using our computational approach. This is why such terms as *e.g.* $3d^3[^4F]4s4p[^3P^o]\ ^2F^o$ were not included in this study and require separate consideration.

For the states $3d^4 4s$, the 3*d*–4*s* intershell correlation is manifested by the large contributions of the $3d^3 4p^2$ (not shown in Table 3 but available for other terms) and $3d^3 4p4f$ configurations corresponding to the dipole interaction $3d4s–4p^2$ and $3d4s–4p4f$, respectively. For the same reason, the intershell correlation 3*d*–4*p* is important for the states with the configuration $3d^4 4p$. The large contribution of the correlation configuration $3d^3 4p5s$ in the $3d^4 4p$ states is caused by the dipole interaction 3*d*4*p*–4*p*5*s*. The correlation effects between two valence electrons are exhibited by the large mixing of the correlation configurations $3d^3 4s5p$ and $3d^3 4p4d$ with the $3d^3 4s4p$ states.

**Table 4.** Excitation energies for selected levels including relativistic corrections.

| Configuration | Term | *J* | $E_{exc}$, eV [38] | $E_{exc}$ MCHF, eV | $\Delta E_{exc}$, eV |
|---|---|---|---|---|---|
| $3d^3 4s^2$ | a $^4F$ | 3/2 | 0.000 | 0.000 | 0.000 |
| | | 5/2 | 0.017 | 0.020 | 0.003 |
| | | 7/2 | 0.040 | 0.049 | 0.008 |
| | | 9/2 | 0.069 | 0.085 | 0.016 |
| $3d^4[^5D]4s$ | a $^6D$ | 1/2 | 0.262 | 0.569 | 0.307 |
| | | 3/2 | 0.267 | 0.575 | 0.308 |
| | | 5/2 | 0.275 | 0.586 | 0.311 |
| | | 7/2 | 0.287 | 0.601 | 0.314 |
| | | 9/2 | 0.301 | 0.620 | 0.319 |
| $3d^4[^5D]4s$ | a $^4D$ | 1/2 | 1.043 | 1.477 | 0.434 |
| | | 3/2 | 1.051 | 1.487 | 0.436 |
| | | 5/2 | 1.064 | 1.502 | 0.439 |
| | | 7/2 | 1.081 | 1.525 | 0.444 |
| $3d^3 4s^2$ | a $^4P$ | 1/2 | 1.183 | 1.446 | 0.262 |
| | | 3/2 | 1.195 | 1.461 | 0.267 |
| | | 5/2 | 1.218 | 1.487 | 0.269 |
| $3d^3[^4F]4s4p[^3P^o]$ | z $^6G^o$ | 3/2 | 2.029 | 2.465 | 0.436 |
| | | 5/2 | 2.040 | 2.477 | 0.437 |
| | | 7/2 | 2.055 | 2.493 | 0.438 |
| | | 9/2 | 2.074 | 2.514 | 0.440 |
| | | 11/2 | 2.097 | 2.540 | 0.442 |
| | | 13/2 | 2.125 | 2.570 | 0.446 |
| $3d^3[^4F]4s4p[^3P^o]$ | z $^6D^o$ | 1/2 | 2.242 | 2.701 | 0.458 |
| | | 3/2 | 2.247 | 2.709 | 0.461 |
| | | 5/2 | 2.256 | 2.722 | 0.465 |
| | | 7/2 | 2.269 | 2.740 | 0.471 |
| | | 9/2 | 2.286 | 2.764 | 0.477 |
| $3d^5$ | a $^6S$ | 5/2 | 2.505 | 2.962 | 0.458 |
| $3d^4[^5D]4p$ | z $^6P^o$ | 3/2 | 3.056 | 4.250 | 1.194 |
| | | 5/2 | 3.066 | 4.264 | 1.198 |
| | | 7/2 | 3.080 | 4.283 | 1.203 |
| $3d^4[^5D]4p$ | z $^4P^o$ | 1/2 | 3.071 | 3.922 | 0.851 |
| | | 3/2 | 3.089 | 3.940 | 0.851 |
| | | 5/2 | 3.116 | 3.971 | 0.855 |

Finally, Table 4 shows the excitation energies for the fine structure levels, calculated in the quasi-relativistic Breit–Pauli approximation. Since the deviation of the theoretical values from the experimental data of NIST [38] for the excited state is in general comparable with the deviation given in Table 1, we presented here only few results for particular terms for each type of the configurations under consideration.

Despite the satisfactory agreement of the calculated excitation energies with the available experimental data, it is important to note the overall good agreement for the difference between the excitation energies of various states. That is, the mutual placement of the calculated energy levels for most of the excited states of neutral vanadium atom corresponds to what is observed in an experiment. This is very important for further study of transitions between levels using the calculated wave functions.

## 4. Conclusions

In this work, we calculated wave functions of the ground and 44 excited states of neutral vanadium atom in scope of the non-relativistic *LS* approximation by using the multi-configuration Hartree–Fock method and configuration interaction approach. The term-dependent non-orthogonal one-electron orbitals were used to construct multi-configuration expansions. Only configurations with significant for a specific term mixing coefficients were included into expansions that made it possible to take into account main correlation effects and at the same time to keep acceptable size of the configuration expansion, which is about ~350 on average and maximum of ~650 configurations. The calculated excitation energies are in a satisfactory agreement with the experimental values averaged by fine structure levels [38], and the median difference is about 0.5 eV.

The main correlation contributions for the multi-configuration expansions for each of the five types of electronic configurations under consideration ($3d^3 4s^2$, $3d^4 4s$, $3d^3 4s4p$, $3d^5$ and $3d^4 4p$) were investigated.

The wave functions of the lower levels of neutral vanadium were also calculated in the quasi-relativistic Breit–Pauli approximation and the corresponding energy spectrum was obtained taking into account fine structure splitting of the levels.

The obtained sets of the wave functions can be used in further calculations of low-energy electron scattering by vanadium atom and photoionization processes.

## References


1. Dere K.P., Del Zanna G., Young P.R., and Landi E. CHIANTI – An Atomic Database for Emission Lines. XVII. Version 10.1: Revised Ionization and Recombination Rates and Other Updates. *Astrophys. J. Suppl. Ser.* 2023. **268**, No 2. https://doi.org/10.1103/10.3847/1538-4365/acec79.
2. Hinkel N.R., Timmes F.X., Young P.A. *et al.* Stellar Abundances in the Solar Neighborhood: The Hypatia Catalog. *Astron. J.* 2014. **148**, No 3. https://doi.org/10.1088/0004-6256/148/3/54.
3. Matteucci F. Introduction to galactic chemical evolution. *J. Phys.: Conf. Ser.* 2015. **703**. P. 012004. https://doi.org/10.1088/1742-6596/703/1/012004.
4. Rybizki J., Just A., Rix H.-W. Chempy: A flexible chemical evolution model for abundance fitting. *Astron. Astrophys.* 2017. **605**. P. A59. https://doi.org/10.1051/0004-6361/201730522.
5. Jofré P., Heiter U., Soubiran C. Accuracy and precision of industrial stellar abundances. *Annu. Rev. Astron. Astrophys.* 2019. **57**. P. 571–616. https://doi.org/10.1146/annurev-astro-091918-104509.
6. Young, P.R. Applications of atomic data to studies of the Sun. *Eur. Phys. J. D*. 2024. **78**, No 130. https://doi.org/10.1140/epjd/s10053-024-00915-6.
7. Güzelçimen F., Er A., Öztürk I.K. *et al.* Investigation of the hyperfine structure of weak atomic Vanadium lines by means of Fourier transform spectroscopy. *J. Phys. B*. 2015. **48**, No 11. P. 115005. https://doi.org/10.1088/0953-4075/48/11/115005.
8. Barklem P.S. Accurate abundance analysis of late-type stars: advances in atomic physics. *Astron. Astrophys. Rev*. 2016. **24**, No 9. https://doi.org/10.1007/s00159-016-0095-9.
9. Colón C., de Andrés-García M.I., Isidoro-García L. and Moya A. Theoretical stark broadening parameters for UV–blue spectral lines of neutral vanadium in the solar and metal-poor star HD 84937 spectra. *Atoms.* 2020. **8**, No 4. P. 64. https://doi.org/10.3390/atoms8040064.
10. Finkenthal M., Bell R.E., Moos H.W., and TFR Group. Forbidden (M1) lines in the spectra of titanium, vanadium, chromium, iron, and nickel observed in a tokamak plasma. *J. Appl. Phys.* 1984. **56**. P. 2012–2016. https://doi.org/10.1063/1.334243.
11. Kovtun Yu.V., Kuprin A.S., Shapoval A.N. *et al.* Optical emission spectroscopy of vanadium cathodic arc plasma at different nitrogen pressure. *J. Appl. Phys*. 2023. **134**. P. 243301. https://doi.org/10.1063/5.0177931.
12. Muroga T., Chen J.M., Chernov V.M. *et al.* Present status of vanadium alloys for fusion applications. *J. Nucl. Mater.* 2014. **455**. P. 263–268. https://doi.org/10.1016/j.jnucmat.2014.06.025.
13. Jiang S.-N., Zhou F.-J., Zhang G.-W. *et al*. Recent progress of vanadium-based alloys for fusion application. *Tungsten*. 2021. **3**. P. 382–392. https://doi.org/10.1007/s42864-021-00107-4.
14. Butt L., Dickinson-Lomas A., Freer M. *et al.* Research and development on vanadium alloys for fusion breeder blanket application. *Fusion Eng. Des*. 2025. **210**. P. 114739. https://doi.org/10.1016/j.fusengdes.2024.114739.
15. Ninomiya H., Abe M., Takashima N. Laser action of optically pumped atomic vanadium vapor. *Appl. Phys. Lett.* 1991. **58**. P. 1819–1821. https://doi.org/10.1063/1.105242.

16. Yoshida H., Takashima N., Ninomiya H. New laser action of optically pumped atomic vanadium vapor. *J. Appl. Phys.* 1992. **71**. P. 1044–1045. https://doi.org/10.1063/1.350395.
17. Ninomiya H., Yoshida H., Takashima N. Temporal behavior of population densities of V atoms in an optically pumped V vapor laser. *J. Appl. Phys.* 1992. **71**. P. 3181–3185. https://doi.org/10.1063/1.350960.
18 Ganeev R.A., Resonance Enhancement of Harmonics in Metal-Ablated Plasmas: Early Studies, Chap. 4 in: *Resonance Enhancement in Laser-Produced Plasmas*. P. 139–211. John Wiley & Sons, Inc., 2018. https://doi.org/10.1002/9781119472346.ch4.
19. Zatsarinny O. BSR: B-spline atomic R-matrix codes. *Comput. Phys. Commun.* 2006. **174**, No 4. P. 273–356. https://doi.org/10.1016/j.cpc.2005.10.006.
20. Gedeon V., Gedeon S., Lazur V. *et al.* Low-energy outer-shell photo-detachment of the negative ion of aluminum. *J. Phys. B*. 2018. **51**, No 3. P. 035004. https://doi.org/10.1088/1361-6455/aa9c37.
21. Gedeon V.F., Lazur V.Yu., Gedeon S.V., Yegiazarian O.V. Resonances in the electron scattering from a calcium atom. *J. Phys. Stud.* 2022. **26**, No 1. P. 1301–1319. https://doi.org/10.30970/jps.26.1301.
22. Gedeon V.F., Lazur V.Yu., Gedeon S.V., Yegiazarian O.V. Resonance structure of cross-sections of slow-electron scattering by calcium atom. *Ukr. J. Phys.* 2022. **67**, No. 3. P. 161–182. https://doi.org/10.15407/ujpe67.3.161.
23. Zatsarinny O., Bartschat K., Gedeon S. *et al.* Low-energy electron scattering from Ca atoms and photodetachment of $Ca^-$. *Phys. Rev. A.* 2006. **74**, No 5. P. 052708. https://doi.org/10.1103/PhysRevA.74.052708.
24. Gedeon V., Gedeon S., Lazur V. *et al.* Electron scattering from silicon. *Phys. Rev. A.* 2012. **85**, No 2. P. 022711. https://doi.org/10.1103/PhysRevA.85.022711.
25. Gedeon V., Gedeon S., Lazur V. *et al.* B-spline R-matrix-with-pseudostates calculations for electron-impact excitation and ionization of fluorine. *Phys. Rev. A.* 2014. **89**. No 5. P. 052713. https://doi.org/10.1103/PhysRevA.89.052713.
26. Gedeon V., Gedeon S., Lazur V. *et al.* B-spline R-matrix-with-pseudostates calculations for electron collisions with aluminum. *Phys. Rev. A.* 2015. **92**, No 5. P. 052701. https://doi.org/10.1103/PhysRevA.92.052701.
27. Froese Fischer C., Godefroid M., Brage T. *et al*. Advanced multiconfiguration methods for complex atoms: I. Energies and wave functions. *J. Phys. B*. 2016. **49**. P.182004. https://doi.org/10.1088/0953-4075/49/18/182004.
28. Scharf O., Gaigalas G. Large scale multi-configuration Hartree–Fock calculation of the hyperfine structure of the ground state of vanadium. *Cent. Eur. J. Phys*. 2006. **4**, No 1. P. 42–57. https://doi.org/10.1007/s11534-005-0005-7.
29. Osanai Y., Ishikawa H., Miura N., Noro T. Excitation energies, electron affinities and ionization potentials of the transition metals V, Cr and Mn. *Theor. Chem. Acc.* 2001. **105**. P. 437–445. https://doi.org/10.1007/s002140000234.
30. Cowan R.D. *The Theory of Atomic Structure and Spectra*. Univ. California Press, Berkeley, CA, 1981.
31. Thorne A.P., Pickering J.C., Semeniuk J. The spectrum and term analysis of V I. *Astrophys. J. Suppl. Ser.* 2011. **192**. No 1. P. 11. https://doi.org/10.1088/0067-0049/192/1/11.
32. Saloman E.B., Kramida A. Critically evaluated energy levels, spectral lines, transition probabilities, and intensities of neutral vanadium (V I). *Astrophys. J. Suppl. Ser.* 2017. **231**, No 2. P. 18. https://doi.org/10.3847/1538-4365/aa7e2a.
33. Smirnov Y.M. Excitation cross sections for a vanadium atom. *J. Appl. Spectrosc.* 1995. **62**, P. 996–1000. https://doi.org/10.1007/BF02606746.
34. Smirnov Y.M. Excitation of $^4$G°, $^4$H°, and $^4$I° levels of vanadium atom by slow electrons. *High Temperature*. 2001. **39**. P. 37–42. https://doi.org/10.1023/A:1004162228700.
35. Krasavin A.Y., Kuchenev A.N., Smirnov Y.M. Excitation cross sections of the vanadium atom. *J. Appl. Spectrosc.* 1982. **36**. P. 575–580. https://doi.org/10.1007/bf00663667.
36. Mel'nikov V.V., Smirnov Yu.M. Excitation of vanadium atoms by electron impact. *Opt. Spectrosc.* 1982. **53**, No 1. P. 27–32.
37. Peterkop R.K. Calculation of excitation cross sections and oscillator strengths for vanadium and manganese atoms. *Opt. Spectrosc.* 1985. **58**, No 1. P. 7–10.
38. Kramida A., Ralchenko Yu., Reader J., and NIST ASD Team (2022). NIST Atomic Spectra Database (ver. 5.10). Available: https://physics.nist.gov/asd.
39. Fischer C.F., Tachiev G., Gaigalas G., Godefroid M.R. An MCHF atomic-structure package for large-scale calculations. *Comput. Phys. Commun.* 2007. **176**, No 8. P. 559–579. https://doi.org/10.1016/j.cpc.2007.01.006.
40. Zatsarinny O., Fischer C.F. A general program for computing angular integrals of the Breit–Pauli Hamiltonian with non-orthogonal orbitals. *Comput. Phys. Commun.* 2000. **124**, No 2–3. P. 247–289. https://doi.org/10.1016/S0010-4655(99)00441-5.
41. Zatsarinny O., Fischer C.F. Atomic structure calculations using MCHF and BSR. *Comput. Phys. Commun.* 2009. **180**, No 11. P. 2041–2065. https://doi.org/10.1016/j.cpc.2009.06.007.
42. Tayal S.S., Zatsarinny O. Collision and radiative parameters for Cr II lines observed in stellar and nebular spectra. *Astrophys. J.* 2019. **888**, No 1. P. 10. https://doi.org/10.3847/1538-4357/ab557b.

**Authors' contributions**

**Gedeon S.V.:** conceptualization, methodology, software, validation, formal analysis, investigation, data curation, writing – original draft, visualization, writing – review & editing.
**Lazur V.Yu.:** conceptualization, methodology, formal analysis, validation, supervision, project administration, writing – review & editing.
**Kochemba A.A.:** investigation, resources, data curation, visualization.

**Authors and CV**

**Sergiy V. Gedeon**, Candidate of Physical and Mathematical Sciences, Researcher at the Department of Theoretical Physics of the Uzhhorod National University. Sergiy Gedeon is co-author of more than 50 scientific publications. His research interests include theoretical physics and theory of electron-atom and electron-ion collisions. https://orcid.org/0009-0004-4041-8716

**Volodymyr Yu. Lazur**, Doctor of Physical and Mathematical Sciences, Leading Researcher, Professor of the Department of Theoretical Physics at the Uzhhorod National University, Ukraine. He is the author of more than 300 scientific publica tions. His main research interests include theoretical physics and theory of ion-atom and ion-molecular collisions. E-mail: volodymyr.lazur@uzhnu.edu.ua, https://orcid.org/0000-0002-6958-1910

**Alisa A. Kochemba**, Junior Researcher at the Department of Theoretical Physics of the Uzhhorod National University, Ukraine. Her research interests include theoretical physics and theory of electron-atom and electron-ion collisions. E-mail: alisa.kochemba@uzhnu.edu.ua, https://orcid.org/0009-0002-2230-5465

**Розрахунки атомної структури нейтрального ванадію**

**С.В. Гедеон, В.Ю. Лазур, А.А. Кочемба**

**Анотація.** Багатоконфігураційний метод Хартрі–Фока у поєднанні з методом взаємодії конфігурацій, що використовує неортогональні орбіталі та *B*-сплайни як базисні функції, було застосовано для вивчення атомної структури нейтрального ванадію. Рівні енергій для основного і 44 нижніх збуджених станів атома було розраховано як в рамках нерелятивістського *LS*-наближення, так і з релятивістськими поправками у наближенні Брейта–Паулі. Результати розрахунків задовільно узгоджуються з наявними експериментальними даними. Отримані набори хвильових функцій можуть бути використані у подальших розрахунках процесів фотоіонізації та розсіяння електронів на атомі ванадію.

**Ключові слова:** атом ванадію, атомна структура, електронна кореляція, взаємодія конфігурацій, неортогональні орбіталі.